Computed Profiles of Compressed Sea-Urchin Eggs with Elastic Membranes

AUTHOR(S):

Yoneda, Mitsuki

CITATION:

Yoneda, Mitsuki. Computed Profiles of Compressed Sea-Urchin Eggs with Elastic Membranes. Zoological Science 1988, 5(3): 553-562

ISSUE DATE:

1988-00

URL:

http://hdl.handle.net/2433/108635

ZOOLOGICAL SCIENCE 5: 553-562 (1988)

Computed Profiles of Compressed Sea-Urchin Eggs with Elastic Membranes

MITSUKI YONEDA

Department of Zoology, Faculty of Science, Kyoto University, Kyoto 606, Japan

ABSTRACT—A computer simulation was made for profiles of compressed sea-urchin eggs with various amounts of elasticity at their surfaces. Fluidity of cytoplasm and negligible bending stress of the surface were assumed *a priori*. Based on the profiles thus calculated, the relation of the force of compression and the degree of flattening was predicted and matched with the observed force and flattening of unfertilized eggs of *Hemicentrotus pulcherrimus*. The experimental data were shown to fit well with the calculated force-deformation curve on the assumption of non-elasticity at the surface. The possibility that the egg surface had an elasticity modulus of 10^3 dyne/cm^2 was precluded.

Whether the surface of sea-urchin eggs is elastic or not has been the subject of a debate between Hiramoto [1-5] and myself [6-8]. Both claims have emerged from experimental data on the force required to compress the egg by the "compression method" originally developed by Cole [9].

When an unfertilized sea-urchin egg with the diameter Z_0 is compressed between a pair of parallel plates with a known force (F), the thickness (Z) of the egg reaches an equilibrium within a few minutes. By measuring the thickness of a single egg under varing amounts of force, we can determine the relation of the force (F) and the thickness ($z=Z/Z_0$) as a "F-z curve" (Fig. 1).

Hiramoto adopted a mathematical procedure different from mine to calculate the tension (T) working at the egg surface from measured values of force (F). This gave rise to the differing views as to the physical nature of the egg surface; Hiramoto [1] converted the measured force into excess internal pressure $P=F/\pi D^2$ by measuring the radius (D) of the circle of cell surface in contact with the plates of compression (Fig. 1). By also measuring the radii of curvatures (R_1 and R_2) of the egg surface, he calculated the meridional and equatorial tensions (T_L and T_T) with two formulae,

$$\pi R_2^2 P = 2\pi R_2 T_L + F \quad \text{and} \quad P = T_L/R_1 + T_T/R_2.$$

Accepted April 20, 1988

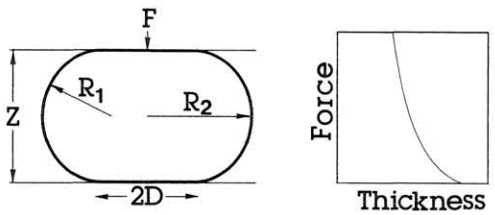

FIG. 1. Sea-urchin egg compressed to thickness (Z) between a pair of parallel plates under force (F) of compression. R_1 and R_2 are radii of the principal curvature of the egg surface at the equator. D is the radius of the circular area in contact with the plate. Typical curve of the force versus flattening of the egg is shown schematically to the right.

Both tensions were found to increase as the egg surface is stretched upon compression, which lead him to claim the presence of elasticity at the egg surface.

The method I adopted equates the work of compression, $-F dZ$, with the work of stretching the surface, $T dS$. Hence $F=T(-dS/dZ)$, or

$$F = \pi T Z_0 (-ds/dz) \qquad (1)$$

where $s=S/S_0$ is the total surface area (S) of the compressed egg divided by the initial surface area, $S_0=\pi Z_0^2$. I calculated the tension (T) by eq. (1) employing an empirical expression of the surface area derived from measured Z, R_1 and R_2, and found that the calculated tension now remains constant in spite of the change in surface area.

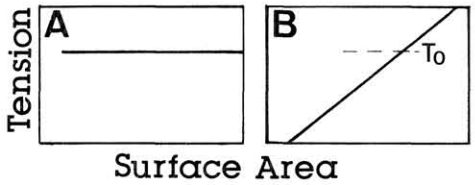

FIG. 2. Conceptual illustration of the relation between the tension and the degree of stretching of the egg surface. A: Non-elastic surface. The tension is independent of the surface area. B: Elastic surface. The tension increases upon surface stretching. T_0 is the initial tension when the egg is a sphere.

Thus I concluded that the egg surface is *not* elastic, a view diametrically opposite to Hiramoto's. Figure 2 is a conceptual illustration of the contrast between the calculated results.

Thus the debate has arisen as to the validity of both procedures. I feel that the term D used by Hiramoto will not be accurately measured because the "angle of contact" is close to 180°. Conversely, Hiramoto (1976) argues that "it is questionable whether $-dS/dZ$ could be determined with a reasonable accuracy" because "increase in surface area dS by compression dZ is very small". Both Hiramoto and I have reinforced our own theories by supplementing with circumstantial evidence, which however, does not logically prove or disprove the validity of either calculation.

I [6, 7] earlier found an analytical solution for the profile of the compressed egg, assuming non-elasticity of the egg surface. The calculated contour coincided with the actual contour of the compressed egg. Calculated values of $-ds/dz$ were also consistent with those derived from measured geometrical parameters. The agreement between the calculation and observation, while supporting the view of non-elasticity of the egg surface, does not prove it however, since an elastic membrane may also show similar contours and similar values of $-ds/dz$.

I recently found a mathematical procedure to derive the profile of elastic shells by numerical calculation. The theoretical contour thus obtained provides a means of directly evaluating the unprocessed raw data of the force versus compression without relying upon the geometrical parameters of the egg, as presented here.

CALCULATION

Mathematical formulation

Since the profile of the compressed egg is axially symmetric, the problem is finding the meridian of the egg by numerical calculation. Four assumptions can be made: that 1) the volume of the egg remains unchanged upon compression, 2) the surface does not resist bending, 3) the inner cytoplasm is fluid, and 4) hydrostatic pressure inside the egg cytoplasm does not affect the egg shape. Based on these assumptions, the egg is looked upon as a thin elastic shell encircling incompressible fluid, to which the classical membrane theory of shells can be applied.

Two kinds of mathematical expressions for balance of forces are known to apply to the thin elastic shell loaded with external forces along the axis, as given by Timoshenko and Woinowsky-Krieger [10]. One is the familiar Laplace formula which relates the internal pressure P with the tensions (T_L and T_T) as

$$P=T_L/R_L+T_T/R_T \tag{2}$$

where T_L is the tension in the direction of the meridian (meridional tension) and T_T (transverse tension) is the tension in the direction perpendicular to T_L (Figs. 3 and 4). R_L is the radius of curvature of the meridian and R_T is the radius of curvature in the direction perpendicular to R_L and, by the theory of differential geometry, equal to the line segment normal to the meridian cut by the symmetry axis.

Another expression for axially loaded shell is

$$d/d\varphi\,(T_LX)-T_TR_L\cos\varphi+YR_LX=0$$

[eq. (f) on page 434 in Timoshenko and Woinowsky-Krieger [10]]. In the case of compressed shells, the term Y, expressing the force acting tangentially to the shell, is null. Defining the orthogonal coordinates (x−y) as shown in Figure 3 in which the line $x=0$ denotes the symmetry axis, we obtain $dX/d\varphi=R_L\cos\varphi$. Hence,

$$d/dX(XT_L)=T_T \tag{3}$$

The calculations to follow are to find the profile of the egg which satisfies both eqs. (2) and (3). To

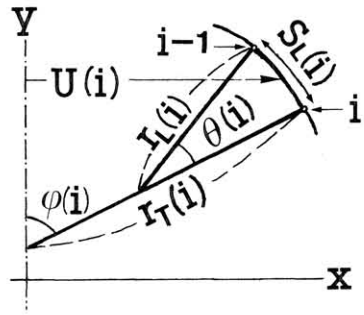

FIG. 3. Geometric parameters describing the compressed shell. Parameters R_L and R_T in eq. 2 correspond to $r_L(i)$ and $r_T(i)$ in this figure.

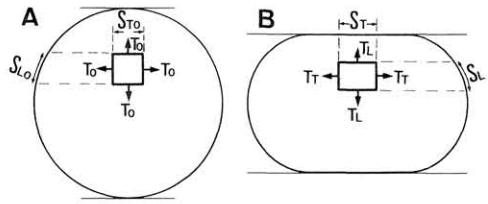

FIG. 4. Rectangular surface element. Its meridional (S_{L0}) and transverse (S_{T0}) dimensions in the spherical shell change to $S_L \times S_T$ upon compression. The initial tension working at element T_0 changes to T_L and T_T in the meridional and transverse directions, respectively.

begin with, let us suppose a rectangular surface element of the shell with the meridional and tranverse dimensions S_{L0} and S_{T0} (Fig. 4A). When the shell is a sphere, the meridional and tranverse tensions coincide at T_0. Compression will change the dimension of the element to S_L and S_T (Fig. 4B). "Relative elongation" E_L and E_T of the element, are defined here as

$$E_L=(S_L-S_{L0})/S_{L0}, \quad E_T=(S_T-S_{T0})/S_{T0} \qquad (4)$$

Denoting the thickness and Young's modulus of the shell by h and E respectively, T_L is given as

$$T_L=T_0+\frac{E_L+sE_T}{(1+E_L)(1+E_T)}\cdot\frac{Eh}{1-s^2}$$

where s is the Poisson ratio of the material of the shell and usually assigned with the value of 0.5 for rubbery materials. Now the term "elasticity index", $Q=Eh/(1-s^2)/T_0$, which represents the magnitude of elasticity (E) relative to the initial tension T_0, is defined. Then, letting $t_L=T_L/T_0$,

$$t_L=T_L/T_0=1+\frac{E_L+0.5E_T}{(1+E_L)(1+E_T)}Q \qquad (5)$$

Similarly, $t_T(=T_T/T_0)$ is calculated by

$$t_T=T_T/T_0=1+\frac{E_T+0.5E_L}{(1+E_T)(1+E_L)}Q \qquad (6)$$

All parameters used in calculations are expressed in their relative values, $z=Z/Z_0$, $t_L=T_L/T_0$, $t_T=T_T/T_0$, $r_L=R_L/R_0$, $r_T=R_T/R_0$, $d=D/R_0$ and $p=P\,R_0/T_0$, where R_0, Z_0, T_0 are the initial radius, diameter and tension, respectively, when the shell is a sphere. Expressing eqs. (2) and (3) by these parameters, we have

$$p=t_L/r_L+t_T/r_T \qquad (7)$$

and

$$d/dx(x\,t_L)=dt_L/dx+t_L=t_T \qquad (8)$$

Starting profile

Calculation of the profile of the compressed shell was started by assuming a semicircular contour at the free surface, and by assigning a proper value of $d(=D/R_0)$ so that the volume encompassed by the shell retains the volume of the sphere with a unit radius. The boundary between the surface in contact with the plate and the free surface will be called "the border", hereafter.

Fine detail of the shell was described by positions in orthogonal co-ordinates of "nodes" which divide the meridian into 48 "segments" (Fig. 5). The nodes are serially numbered from 0 (pole) to

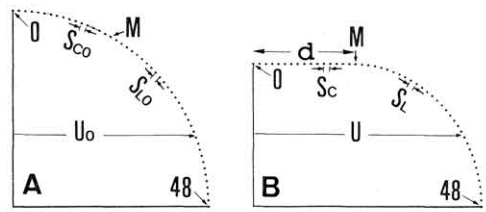

FIG. 5. Form of meridians of the initial (A) and compressed (B) shells defined by node nos. 00 to 48. The node at the border is "node M". Initial lengths of "segments" delimited by adjacent nodes are S_{C0} (at the contacting surface) and S_{L0} (at the free surface). On compression, they change to S_C and S_L, respectively. U_0 and U are the position on the X-coordinates of the center of the segment.

48 (equator). Initially, they were properly spaced along the surface of the compressed shell so as to allocate either one of the nodes on the border. This is denoted by node M. Initial spacing of the nodes is S_C on the surface contacting the plate and S_L on the free surface (Fig. 5B). Such a distribution of the nodes on the compressed shell was transcribed back to the initial sphere, accommodating the spacing to different meridional lengths between the compressed and spherical shells, so that the spacing among nodes 0 to M (S_{C0}) and the spacing among nodes M to 48 (S_{L0}) retain the ratio S_C/S_L.

The original positions of the center of each segment on the X-coordinate (U_0 in Fig. 5) in the sphere varies among segments and is expressed as $U_0(i)$ (i=0 to 48). The corresponding value for the position in the compressed profile is U(i). Due to the axial symmetry of the shell, the ratio $U(i)/U_0(i)$ is numerically equal to S_T/S_{T0} (cf. eq. (4)) which is the rate of stretching of the rectangular element shown in Figure 4 along the transverse direction. In routine calculations, E_T was given as $U(i)/U_0(i)$.

The nodes 0 to M at the contacting surface were defined by their positions in orthogonal coordinates as x(i) and y(i), but nodes M+1 to 48 at the free surface were primarily defined by $r_L(i)$ and $\theta(i)$ for convenience in calculation, and x(i) and y(i) for i=M+1 to 48 were given successively by $r_L(i)$ and $\theta(i)$ (see Fig. 3), starting from node M (border) as

$$\varphi(i)=\varphi(i-1)+\theta(i)$$
$$x(i)=x(i-1)+r_L(i)\,[\sin\varphi(i)-\sin\varphi(i-1)]$$
$$y(i)=y(i-1)+r_L(i)\,[\cos\varphi(i)-\cos\varphi(i-1)]$$

$S_L(i)$ is directly obtained as $\theta(i)r_L(i)$.

Iteration for fine adjustment of the profile

The compressed shell was defined in the foregoing section by rather arbitrary parameters under given flattening (=z) and elasticity index (Q). This is the starting model to be examined for local balance of forces.

First, the rates of stretching (E_L and E_T) of each segment obtained by eq. (4) were used to calculate the local tensions $t_L(i)$ and $t_T(i)$ by eqs. (5) and (6). The pair of $t_L(i)$ and $t_T(i)$ determined for each segment was then examined as to whether they satisfy both eqs. (7) and (8), which are two fundamental expressions of the balance of forces in elastic shells under compression, by calculating imbalance between the lefthand and righthand sides of the equations under given $t_L(i)$ and $t_T(i)$. According to the amount of the imbalance, necessary adjustments were made for parameters $r_L(i)$, $\theta(i)$, or d to improve the profile of the shell. Iteration of the adjustment is explained in the Appendix. The whole procedure was repeated using the renewed parameters $r_L(i)$, $\theta(i)$ and d until the calculated profile substantially satisfied the conditions predicted by eqs. (7) and (8).

RESULTS

The profile of the shells under a given degree (z) of compression is determined by the elasticity index $Q=Eh/(1-s^2)/T_0$ as the only parameter. Hiramoto (1963) calculates Young's modulus (E) for the surface membrane of unfertilized eggs of *Hemicentrotus pulcherrimus* as 1.2×10^3 dyne/cm^2 when the membrane thickness (h) is 3.1 μm, and the initial tension T_0 is 0.032 dyne/cm. These values give the value of Q as 16. The calculations were, therefore, made of the profile of a shell compressed from z=0.90 down to 0.40, and assigned with varying elasticity indices (Q) ranging from 0 (no elasticity) to 16. The results are summarized in Table 1 and show the geometrical parameters of the compressed shell. In real eggs, the force (F) of compression is counterbalanced by the force $F=\pi PD^2$ due to internal pressure (P), and since πPD^2 can be written as $(pd^2/2)\pi T_0Z_0$, the value of $pd^2/2$ in Table 1 is identical to $(-ds/dz)$ in eq. (1). The present values of $pd^2/2$ for Q=0 were found to coincide with $-ds/dz$ (not shown here) derived in a previous paper [11] by an analytical solution of the profile.

Typical examples of the contour of the shell under compression (z) in 4 steps for Q=0 and 16 are drawn in Figure 6. The contours in the presence of elasticity (shown by circles) tend to become flatter near the equatorial surface than the contour in the absence of elasticity (lines), resulting in a diminished largest diameter of the shell. Conversely, the contours of the elastic shell exhibit steeper curvatures at the region near the boundary

TABLE 1. Geometric parameters of elastic shells under compression

z	u	d	p	$pd^2/2$	z	u	d	p	$pd^2/2$
Q = 0					Q = 5				
.90	1.022	0.215	2.046	0.047	.90	1.018	0.247	2.080	0.063
.85	1.038	0.284	2.082	0.083	.85	1.031	0.325	2.153	0.113
.80	1.057	0.350	2.125	0.130	.80	1.048	0.397	2.254	0.177
.75	1.079	0.416	2.178	0.188	.75	1.069	0.466	2.387	0.259
.70	1.104	0.484	2.243	0.262	.70	1.093	0.534	2.562	0.365
.65	1.132	0.554	2.321	0.356	.65	1.122	0.602	2.788	0.505
.60	1.166	0.628	2.417	0.476	.60	1.156	0.672	3.080	0.696
.55	1.205	0.708	2.536	0.635	.55	1.196	0.746	3.458	0.963
.50	1.250	0.794	2.683	0.846	.50	1.243	0.826	3.950	1.348
.45	1.304	0.890	2.869	1.136	.45	1.299	0.915	4.596	1.924
.40	1.370	0.997	3.110	1.546	.40	1.365	1.016	5.453	2.815
Q = 1					Q = 10				
.90	1.021	0.222	2.053	0.050	.90	1.015	0.270	2.112	0.077
.85	1.037	0.293	2.096	0.090	.85	1.027	0.354	2.225	0.139
.80	1.055	0.361	2.151	0.140	.80	1.043	0.430	2.385	0.221
.75	1.076	0.428	2.220	0.203	.75	1.063	0.501	2.602	0.326
.70	1.101	0.495	2.306	0.283	.70	1.087	0.568	2.889	0.465
.65	1.130	0.566	2.414	0.386	.65	1.116	0.633	3.264	0.654
.60	1.163	0.639	2.549	0.520	.60	1.151	0.699	3.751	0.916
.55	1.202	0.718	2.720	0.700	.55	1.191	0.768	4.388	1.293
.50	1.248	0.803	2.936	0.946	.50	1.239	0.843	5.222	1.853
.45	1.303	0.897	3.214	1.293	.45	1.296	0.927	6.325	2.715
.40	1.368	1.003	3.578	1.800	.40	1.364	1.024	7.798	4.085
Q = 2					Q = 16				
.90	1.020	0.229	2.060	0.054	.90	1.013	0.291	2.152	0.091
.85	1.035	0.302	2.110	0.096	.85	1.024	0.381	2.315	0.167
.80	1.053	0.371	2.177	0.149	.80	1.039	0.460	2.551	0.269
.75	1.074	0.438	2.262	0.271	.75	1.058	0.531	2.873	0.404
.70	1.099	0.506	2.370	0.303	.70	1.082	0.596	3.297	0.585
.65	1.128	0.576	2.507	0.416	.65	1.111	0.658	3.850	0.832
.60	1.161	0.649	2.682	0.564	.60	1.146	0.719	4.570	1.182
.55	1.201	0.726	2.904	0.766	.55	1.188	0.783	5.513	1.691
.50	1.247	0.810	3.189	1.047	.50	1.237	0.854	6.755	2.461
.45	1.301	0.903	3.560	1.451	.45	1.294	0.934	8.404	3.665
.40	1.367	1.008	4.047	2.053	.40	1.363	1.028	10.614	5.610

z: thickness, u: largest diameter, d: radius of contacting area,
p: internal pressure, Q: elasticity index, $Eh/(1-s^2)/T_0$

than does the non-elastic shell. The calculated radius of the area of contact increased as Q increased. This character of the elastic shell was qualitatively identical to the behaviour of a real tennis ball filled with water under compression [7], when the value of Q was expected to be much higher than 16.

Such a definite and systematic dissimilarity be-

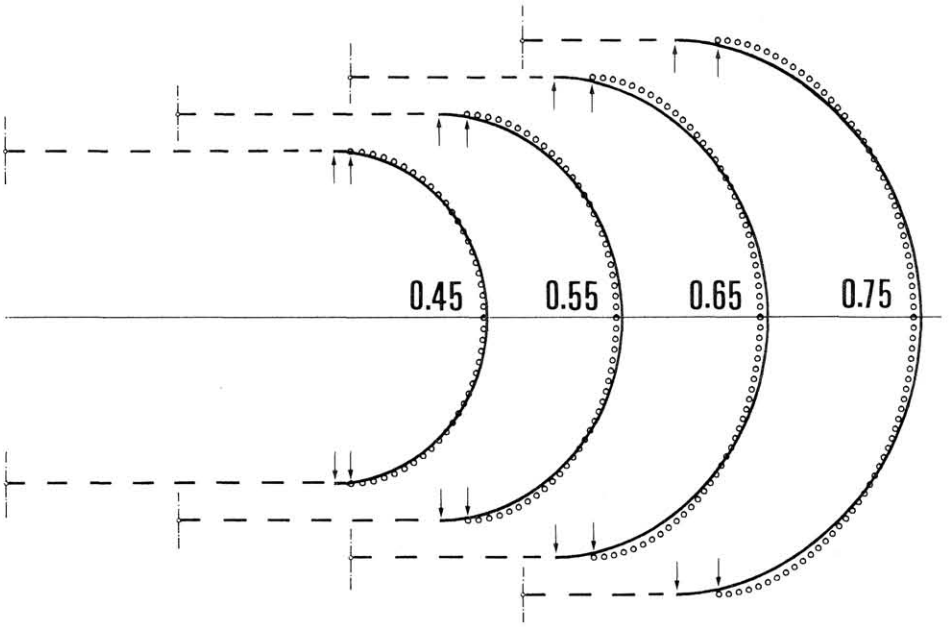

FIG. 6. Calculated contours of elastic and non-elastic shells. Numerals indicate relative thickness (z). Short dot-dash lines indicate the axes of the shells. Solid lines: Non-elastic surface (Q=0). Circles: Elastic surface (Q=16). Arrows point to the border between the contacting and free surface.

TABLE 2. Force of compression measured in unfertilized eggs of *Hemicentrotus pulcherrimus* (assembled by Prof. Yukio Hiramoto)

Relative thickness (Z)	0.90	0.80	0.70	0.60
Force of compression (F) ($\times 10^{-4}$ dyne)	0.90	2.25	4.60	8.75

tween the two contours is, however, not very large. As is evident from Table 1, the largest diameters differ, at the most, by only 2% (at z=0.70). Matching these contours with the actual contour of the real eggs would require high-quality pictures of several numbers of sea urchin eggs under compression before a fair judgement could be formed.

Yet Table 1 provides another means of testing the presence or absence of elasticity by using the values of $pd^2/2$ as a proportionality factor for predicting the force of compression (F). Prof. Yukio Hiramoto of the University of the Air kindly supplied me with his data on the force required to compress unfertilized eggs of *Hemicentrotus pulcherrimus* (Table 2). The calculated values of $pd^2/2$ for each degree of compression were multiplied by a certain factor (mathematically equal to T_0Z_0) so as to get the best fit for the data (Fig. 7). As in the case of matching contours, here, too, the predicted forces of compression of elastic and non-elastic shells were not very different, both fitting substantially well with the observed data. This is not entirely unexpected, however. In such a range ($z \geqq 0.6$) of mild compression, the surface is only slightly stretched and the elasticity, if any, will not largely affect the issue.

Data presented in my earlier paper [6] will now be utilized since it includes 50 readings on 11 unfertilized eggs of *Hemicentrotus pulcherrimus* (Table 3) covering the range of compression down to 0.485. For each egg, the force of compression at z=0.75 was estimated by proper intrapolation of measured forces, as indicated in Table 1 under the

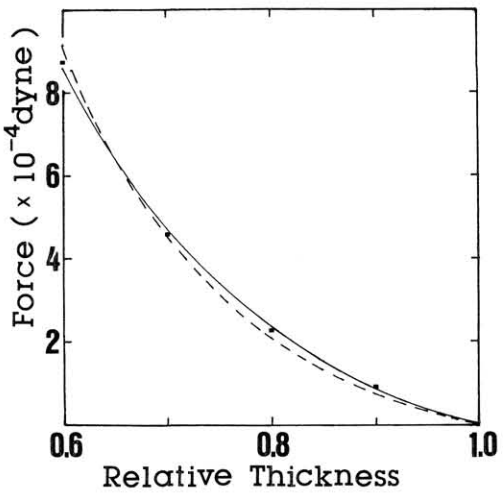

FIG. 7. Calculated force-deformation curves fitted to observed force (dots) at z=0.90 to 0.60. Data obtained from Prof. Yukio Hiramoto. Solid line: Non-elastic (Q=0) surface. Broken line: Elastic surface (Q=16).

column "F_{75}". To even out the variation among eggs, the measured forces were normalized so that the estimated values of F_{75} would come to unity. The normalized forces were plotted on a logarithmic scale against the degree of flattening (Fig. 8) in order to critically examine the F−z curve rather than the absolute values of force. The calculated force for the shells with or without elasticity (Q=0 and 16) were similarly normalized to have a unit force at z=0.75 and also plotted on the logarithmic scale. A substantial divergence in the calculated forces between elastic and non-elastic shell was noted. Plots of measured forces are now scattered around the theoretical curve for Q=0 (solid line) and favors the claim of non-elasticity of the membrane. Owing to the nature of logarithmic plotting, the points representing small forces for mild compression (z=0.75 to 0.9) are widely scattered, yet they are located closer to the solid line (Q=0) than to the broken line (Q=16). Both calculated curves happen to be quite linear on a logarithmic

TABLE 3. Force of compression (F) and thickness (Z) measuerd in unfertilized eggs of *Hemicentrotus pulcherrimus*

Egg							F_{75}	Z_0
1	0.20	0.53	1.16	1.66	2.21	3.27	0.68	93.0
	(.900)	(.795)	(.680)	(.595)	(.550)	(.485)		
2	0.26	0.64	0.90	1.58	2.50		0.53	94.0
	(.860)	(.725)	(.665)	(.570)	(.495)			
3	0.64	1.15	1.79	2.56			0.68	98.0
	(.780)	(.680)	(.580)	(.530)				
4	0.38	0.92	1.56	2.27			0.75	97.5
	(.845)	(.715)	(.630)	(.575)				
5	0.15	0.62	0.89	1.35	1.81		0.49	97.0
	(.855)	(.735)	(.645)	(.590)	(.535)			
6	0.48	0.99	1.52	2.13			0.84	95.5
	(.830)	(.725)	(.665)	(.605)				
7	0.33	0.56	0.85	1.61			0.51	93.5
	(.825)	(.720)	(.670)	(.570)				
8	0.20	0.43	0.70	1.05	1.51	2.10	0.58	92.0
	(.870)	(.770)	(.705)	(.645)	(.605)	(.560)		
9	0.31	0.67	1.00	1.63	2.33		0.55	93.0
	(.840)	(.735)	(.650)	(.570)	(.510)			
10	0.32	0.59	1.20	2.02			0.66	97.0
	(.860)	(.760)	(.650)	(.580)				
11	0.29	0.67	0.95				0.37	95.0
	(.780)	(.665)	(.600)					

Taken from the data presented in [6]. Upper rows: Force in 10^{-3} dyne. Lower rows in parentheses: Relative thickness ($z=Z/Z_0$). Force to compress the egg to z=0.75 estimated by proper intrapolation is shown under "F_{75}". Z_0: initial diameter(μm).

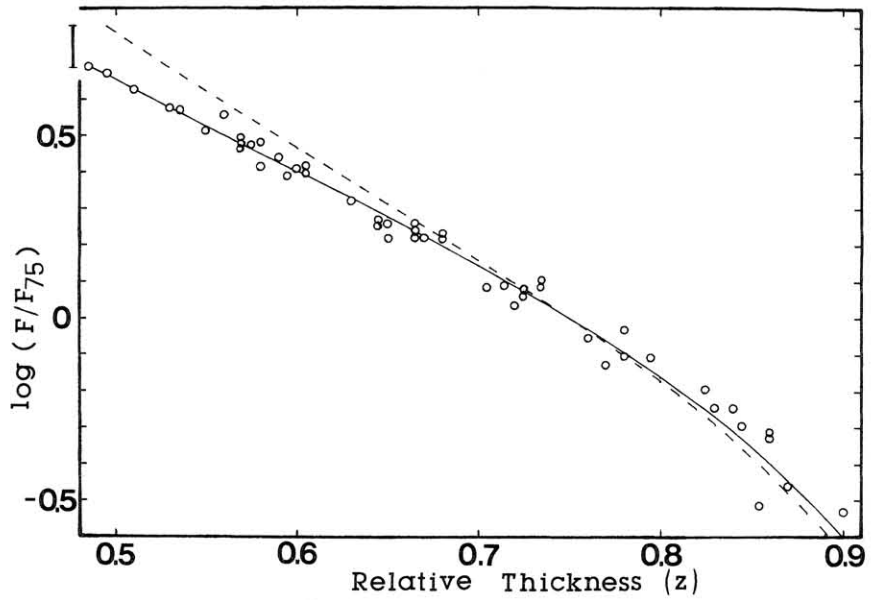

FIG. 8. Data measured at z=0.90 to 0.485 and the calculated forces for Q=0 (solid line) and Q=16 (broken line) are plotted on a logarithmic scale against the relative thickness, and normalized so that the values at z=0.75 ("F_{75}") come to unity. The scale bar at the upper-left corner indicates a 30% change of force.

TABLE 4. Culculated slopes of the log F–Z/Z_0 curve

Q	0	1	2	5	8	12	16
slope	−2.60	−2.66	−2.72	−2.85	−2.95	−3.04	−3.12

Calculated force at z=0.75, 0.70, 0.65, 0.60, 0.55, 0.50 were linearized.

scale in the low range of z (<0.75). The slopes of the (log F)−z curves are shown in Table 4. On the other hand, the slope of the linear regression curve for 36 points (in common logarithm) measured in the range of z from 0.75 to 0.48 was found to be −2.57. The error variance $S^2=(S_{yy}-S_{xy}^2/S_{xx})/(n-2)$ of the slope was 0.00065 where the "sums of products", S_{xx}, S_{xy} and S_{yy} were 0.178, −0.459 and 1.202, respectively, and n=36. Based on these parameters, the probable range of the slope is -2.57 ± 0.17 ($t\sqrt{S^2/S_{xx}}=2.7\times0.061=0.17$) at $p<0.01$. Comparison with the calculated slopes precludes the possibility that the surface of unfertilized sea-urchin eggs has elasticity index as high as 16, or the Young's modulus of 10^3 dyne/cm^2 as claimed by Hiramoto [1]. A small amount of elasticity up to Q=2 is marginally probable, but making a distinction between non-elasticity and elasticity as low as Q=2 (Young's modulus of 10^2 dyne/cm^2) appears very difficult using experimental data from the compression method. Thus, the data presented do not support the presumption of elasticity.

REMARKS

The present paper reports success in calculating the profile of spherical shells with given elasticity, which could serve to simulate deformed animal cells. The present calculation was based on simplifying assumptions. Among them, the assumptions that there is no bending stress in the membrane and that the inner cytoplasm is fluid should be kept in mind when simulating the calculated profile with living cells. As for unfertilized eggs of the sea-urchin, I earlier estimated that the bending stress of the membrane would be negligible in the compression experiment [6]. Measurement of the

viscoelasticity of the cytoplasm of unfertilized sea-urchin eggs by Hiramoto [12] indicates that deformation of the cytoplasm will not create any permanent stress. Thus, I believe that the present calculation will apply at least to unfertilized sea urchin eggs.

Although the present study precluded the presence of elasticity as high as 10^3 dyne/cm^2 based on Hiramoto's calculation, there are still two sets of data which seem to contradict my claim of non-elasticity. One is the observation of Hiramoto [2] on centrifuged sea-urchin eggs, and the other is my own experience with highly compressed sea-urchin eggs [13]. Critical examinations of these data have not yet been performed.

ACKNOWLEDGMENT

I wish to express my gratitude to Prof. Yukio Hiramoto of the University of the Air who kindly provided me with his data on the compression experiment. I also thank Prof. Susumu Ishii of Waseda University for instructing me on the statistical analysis of measured and calculated slopes of F−z curves. This work was supported in part by a grant from the Ministry of Education, Science and Culture of Japan (61304008, 61490016).

APPENDIX: DETAILS OF THE ADJUSTMENTS

The parameters of the shell were modified by the following five kinds of adjustments.

1) Pressure adjustment (by eq. (7))

The internal pressure p(i) to be held by each segment was calculated by eq. (7) using $t_L(i)$ and $t_T(i)$. The calculated pressures for segments M+1 to 48 were averaged. Based on the premise of uniform pressure in egg cytoplasm (cf. assumption 4 given earlier), the value of $r_L(i)$ for each segment was modified so that the calculated pressures [p(i)] would come closer to their average. Throughout this adjustment, $\theta(i)$ was also modified to compensate for the change in $r_L(i)$ so that $S_L(i)[=r_L(i)\,\theta(i)]$ remains unchanged with the hope that the balance of tensions, which is largely susceptible to change in the length of the segment (S_L), is not drastically disturbed.

2) Tension adjustment at the free surface (by eq. (8))

In numerical calculation, the value dt_L/dx in eq. (8) was replaced by $t_L(i+1)-t_L(i)$ divided by $(x(i+1)-x(i-1))/2$. The balance of forces at each node (M+1 to 48) was examined by putting $t_L(i)$, $t_T(i)$, and x(i) into eq. (8). According to the imbalance thus detected, the position of each node (M+1 to 48) was shifted along the meridian by modifying $\theta(i)$ to improve the balance.

3) Tension adjustment at the contacting surface (by eq. (8))

The tension balance at each node on the contacting surface was adjusted in a procedure similar to adjustment 2 except that the modification was made to x(i) (i=1 to M−1), instead of $\theta(i)$.

4) Tension adjustment at the border (by eq. (8))

Separate adjustments of the tension balance for the contacting and free surfaces (adjustments 2 and 3) will concentrate the imbalance at the border (node M) where the contacting and free surfaces meet. Since the two segments neighboring the border are assigned different resting lengths, S_{C0} and S_{L0}, the adjustment at the border was achieved by shifting the position of node M along the surface of the initial sphere, which inovlves reciprocal changes in S_{C0} and S_{L0} with the accompanying modification of E_L, t_L and t_T. This results in reducing the imbalance between the two segments at the border. This adjustment of the resting lengths induces a subtle disturbance of the balance in all but one (border) nodes which are carried over to subsequent iterations.

5) Volume adjustment

Adjustments 1 and 2 usually change the calculated volume of the shell. To return it to its initial volume, a certain factor was multiplied to all sets of $r_L(i)$ at the nodes M+1 to 48, and x(i) of nodes 1 to M. A modification of the radius d of the contacting surface is performed for this occasion.

The iteration consisting of these 5 separate adjustments, each involving a negative feedback of imbalances to the original parameters $r_L(i)$, $\theta(i)$ and d, was repeated several times until a) the pressures calculated for all segments became uniform within 0.01%, b) tension imbalances between any adjacent segments became less than 0.1% and c) deviation of the volume from unity became less than 10^{-5}. The chief difficulty encountered in such a scheme of "multiple adjustments" was that any

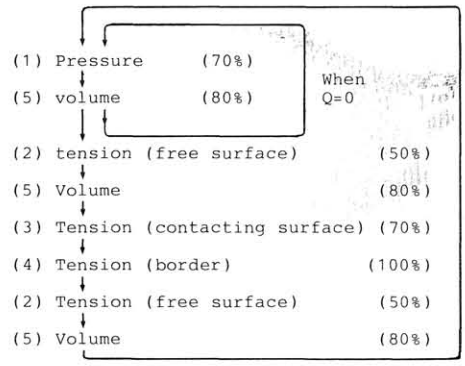

FIG. 9. Iteration of adjustments. Percentages in parentheses are the rate of negative feedback to parameters.

one of the adjustments (pressure, for example) often tended to amplify the imbalance of other aspects (tension for example) resulting in a never-ending oscillation of the calculated profile, even when only moderate changes were imposed on original parameters in a single step of adjustment by limiting the rates of feedback to low levels. A scheme for a successive sequence of adjustments which modified the profile steadily and quickly to its equilibrium was fortunately found after several trials. Figure 9 is the final version of present iteration in which the adopted rates of negative feedback are specified in percentages.

Numerical calculations were automatized by a computer program called "ELAS", written in Basic and adapted to a personal computer (Hitachi S1-40).

REFERENCES

1 Hiramoto, Y. (1963) Mechanical properties of sea urchin eggs. I. Surface force and elastic modulus of the cell membrane. Exp. Cell Res., **32**: 59–75.

2 Hiramoto, Y. (1976) Observations and measurements of sea urchin eggs with a centrifuge microscope. J. Cell. Physiol., **69**: 219–230.

3 Hiramoto, Y. (1970) Rheological properties of sea urchin eggs. Biorheology, **6**: 201–234.

4 Hiramoto, Y. (1976) Mechanical properties of sea urchin eggs. III. Visco-elasticity of the cell surface. Dev. Growth Differ., **18**: 377–386.

5 Hiramoto, Y. (1987) Evaluation of cytomechanical properties. In "Cytomechanics". Ed. by J. Bereiter-Hahn, O. R. Anderson and W.-E. Reif, Springer, Berlin. pp. 31–46.

6 Yoneda, M. (1964) Tension at the surface of sea-urchin eggs. A critical examination of Cole's experiment. J. Exp. Biol., **41**: 893–906.

7 Yoneda, M. (1973) Tension at the surface of sea urchin eggs on the basis of 'liquid drop' concept. Adv. Biolphys., **4**: 153–190.

8 Yoneda, M. (1976) Temperature-dependence of the tension at the surface of sea-urchin eggs. Dev. Growth Differ., **18**: 387–389.

9 Cole, K. S. (1932) Surface force of the Arbacia egg. J. Cell. Comp. Physiol., **1**: 1–9.

10 Timoshenko, S. and Woinowsky-Krieger, S. (1970) Theory of Plates and Shells, McGraw-Hill, New York, 2nd ed., pp. 434.

11 Yoneda, M. (1986) The compression method for determining the surface force. Methods Cell Biol., **27**: 421–434.

12 Hiramoto, Y. (1969) Mechanical properties of the protoplasm of the sea urchin egg. I. Unfertilized egg. Exp. Cell Res., **56**: 201–208.

13 Yoneda, M. (1980) Tension at the highly stretched surface of sea urchin eggs. Dev. Growth Differ., **22**: 39–47.